Hindawi
International Journal of Aerospace Engineering
Volume 2023, Article ID 1983417, 10 pages
https://doi.org/10.1155/2023/1983417

Research Article

Adaptive Terminal Sliding Mode Fault-Tolerant Control of Spacecraft Based on the Left Attitude Error Function of SO(3)

Zhongzhong Zheng, Wei Shang, Zhou Liu, and Yongda Guo

School of Mechanical Engineering, Hubei University of Technology, Wuhan 430068, China

Correspondence should be addressed to Wei Shang; bitshw@126.com

Received 4 May 2023; Revised 11 July 2023; Accepted 24 July 2023; Published 4 August 2023

Academic Editor: Shaoming He

For the problem of spacecraft attitude actuator failure, an adaptive terminal sliding mode fault-tolerant controller (ATSMFTC) based on the differential manifold SO(3) modelling is designed in this paper. First, SO(3) is used to provide a global and unique description of the spacecraft attitude dynamic model. This modelling method not only avoids the problems of singularity and unwinding that exist in traditional modelling methods but also the SO(3) modelling has a simple formulation of the dynamic equations. Then a left attitude error descriptor function is constructed on SO(3) to design an ATSMFTC. This controller is capable of fast and accurate tracking of the time-varying desired attitude. At the same time, it can react quickly to maintain system stability in case of spacecraft attitude actuator failure. The controller designed based on the left attitude error description system of SO(3) has the features of small computational effort and simple design process. Finally, the numerical simulation of the attitude tracking error verifies the feasibility and high efficiency of the controller designed in this paper.

1. Introduction

Attitude control of spacecraft is a key component of the spacecraft control system. The accomplishment of some major space missions requires the consideration of spacecraft attitude control, such as spacecraft rendezvous and docking [1, 2], satellite imaging [3], and spacecraft formation flight [4, 5]. To ensure that the spacecraft serving in orbit can follow the expected trajectory, the spacecraft's attitude should be precisely tracked. However, during the spacecraft mission, the instability of its actuators and the disturbance of the complex external environment may cause the spacecraft attitude actuator to malfunction and deviate from the expected trajectory [6, 7]. Therefore, it is necessary to design a controller to resist these disturbing factors.

Considering the above problems, an idea of fault-tolerant control (FTC) with strong robustness was proposed [8]. In [7], aiming at the buffeting problem generated by the controller, a sliding mode control algorithm without buffeting is designed based on the model. Some remarkable achievements have been made in the design of fault-tolerant controllers for spacecraft attitude [9–11]. A finite-time active FTC scheme was proposed in [12] for spacecraft attitude actuator failures and uncertainties. In [13], an adaptive variable structure FTC was designed based on the method of estimating the fault minimum. In [14], an adaptive fault-tolerant attitude controller based on fixed-time convergence is designed to effectively solve the spacecraft attitude controller parameter uncertainty and external disturbance problems. In [15], an adaptive robust saturation fault-tolerant controller has been designed to effectively solve the problem of FTC of uncertain spacecraft attitude tracking with full-state error constraints.

The control of spacecraft attitude stability is often done for its model uncertainty, and then its dynamical model is modelled by the corresponding attitude description methods. Commonly used spacecraft attitude modelling methods are quaternion [16–19], Euler angles [20], Roglis parameters [21], and differential manifold SO(3) [22, 23]. Most existing spacecraft attitude tolerance controls are based on quaternions [24–27] for controller design. However, quaternions are not unique in describing the attitude, and there is singularity and unwinding in describing the attitude. Compared with quaternions, the differential manifold SO(3) not only describes the spacecraft attitude uniquely and globally but also has no

ambiguity and rewinding [28, 29]. Therefore, in this paper, we design the spacecraft attitude-tolerant controller on the differential manifold SO(3).

Due to these advantages of SO(3), it is widely used in the design of controllers for spacecraft attitude stabilization [30–32]. However, few scholars have combined SO(3) attitude description with fault-tolerant control for fault-tolerant control of spacecraft attitude stabilization. The latest research has been done in [33] by constructing a second-order sliding mode surface on SO(3) and then designing a fault-tolerant controller based on this new sliding mode surface to deal with actuator failures and external disturbances in attitude control. [34] constructed the FTC framework on Lie group SE(3) to solve the large-scale disturbance problem. However, the controllers designed in [33, 34] were studied for the case of the fixed desired attitude. It does not have universal applicability. In contrast, there will be a time-varying desired attitude for spacecraft tracking in real situations. Therefore, in this paper, based on the existing research, the time-varying attitude of spacecraft is tracked by constructing a left attitude error description system on SO(3). The concept of the left attitude error function was first introduced by Bullo in [35]. At the same time, he also proposed the right attitude error function on SO(3). Almost all existing studies are based on the right attitude error function for controller design [36–38]. However, it is difficult for the right error function description system to track the time-varying desired attitude quickly and accurately. In contrast, the left attitude error description system on SO(3) can not only track the desired attitude of the time variation quickly and accurately but also make the controller design less computationally intensive and the control process easier.

In summary, to achieve high accuracy and fast spacecraft attitude time-varying tracking fault-tolerant control, the ASTMFTC is designed in this paper. Firstly, the spacecraft attitude is modelled based on the Lie group SO(3). Then, considering the actuator parameter uncertainties or external disturbances that may still exist after the spacecraft reaches the desired trajectory, a left error description system is constructed on SO(3) to track the spacecraft's time-varying desired attitude effectively. And an adaptive terminal sliding mode control approach is used to design the fault-tolerant controller. The stability of our designed controller is verified by Lyapunov stability. Finally, numerical simulations based on MATLAB simulation software are performed to prove the feasibility of the controllers designed in this paper can be effective. The method proposed in this paper is suitable for the system where the complete attitude can be obtained. If the attitude of the system cannot be directly obtained or observed [39], the control scheme may not be directly applied.

Compared with the existing research results [33, 34], the innovations in this paper are summarized as follows:

The error dynamic equations for the left attitude error function on SO(3) are derived and applied to the design of an ATSMFTC. The designed controller can not only track the time-varying desired attitude quickly and accurately but also can effectively solve the spacecraft attitude actuator failure problem and maintain the system stability.

The rest of this paper is organized as follows: in Section 2, SO(3)-based spacecraft rigid body attitude modelling and left attitude error description are constructed. In Section 3, the adaptive terminal sliding mode fault-tolerant controller is designed. In Section 4, the analysis and illustration of the numerical simulation are performed. In Section 5, the control scheme of this paper is summarized.

2. SO(3)-Based Spacecraft Rigid Body Attitude Modeling and Left Error Description

2.1. Spacecraft Rigid Body Attitude Dynamic Modeling. In this section, the attitude of the spacecraft body in the inertial system can be uniquely described by the nonlinear differential manifold SO(3), as depicted in Figure 1. The attitude $R \in \mathrm{SO}(3)$ is an element in SO(3) and is represented by an orthogonal cosine matrix as follows.

$$\mathrm{SO}(3) = \left\{ R \in \mathbb{R}^{3\times 3} \middle| R^{\mathrm{T}} R = I, \det[R] = 1 \right\}. \tag{1}$$

The attitude kinematics as well as the dynamics of the spacecraft rigid body can be represented by Equation (1) as follows:

$$\begin{cases} \dot{R} = R\widehat{\Omega}, \\ J\dot{\Omega} = -\Omega \times J\Omega + u + d_{\Omega}, \end{cases} \tag{2}$$

where

$$\widehat{\Omega} = \begin{bmatrix} 0 & -\Omega(3) & \Omega(2) \\ \Omega(3) & 0 & -\Omega(1) \\ -\Omega(2) & \Omega(1) & 0 \end{bmatrix}, R \in \mathrm{SO}(3) \tag{3}$$

is the attitude of spacecraft. $\Omega \in \mathbb{R}^3$ is the angular velocity of the spacecraft in the airframe coordinate system. $J \in \mathbb{R}^{3\times 3}$ indicates the rotational moment of inertia. $u \in \mathbb{R}^3$ indicates the total control torque. d_{Ω} is an unknown random disturbance.

2.2. The Left Error Function Description System on SO(3). The concepts of left and right errors were first introduced by Bullo in [35]. By denoting the desired trajectory as $\{R_d(t), t \in \mathbb{R}_+\}$ and the desired velocity as $\{\widehat{\Omega}_d = R_d^T \dot{R}_d\}$ and then using group operations, the left and right attitude errors are defined as

The left error function:

$$R_{e,l} \triangleq R R_d^T. \tag{4}$$

The right error function:

$$R_{e,r} \triangleq R_d^T R. \tag{5}$$

Considering that the left attitude error is easier and more efficient to calculate than the right error when performing

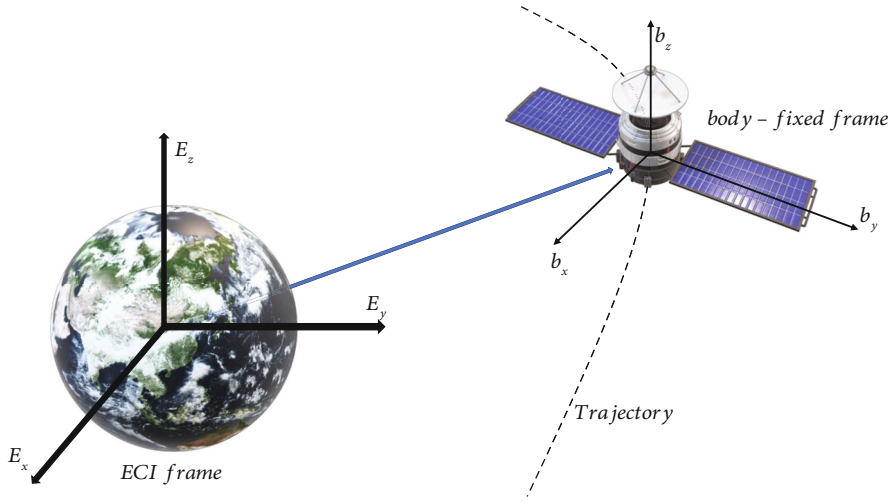

Figure 1: Spacecraft body in the inertial system.

the controller design. So in this paper, we choose to construct the left attitude error on SO(3), which is defined as

$$R_e \triangleq RR_d^T. \tag{6}$$

The error function is then defined as

$$\varphi(R, R_d) \triangleq \phi(R_e), \tag{7}$$

where $\phi : SO(3) \longrightarrow \mathbb{R}_+$ is the error parametrization [34], which is defined as

$$\phi(R_e) = 2 - \sqrt{1 + tr(R_e)}. \tag{8}$$

The error vector is expressed as

$$\begin{cases} e_R = \dfrac{1}{2\sqrt{1 + tr(R_e)}} \left(R_e - R_e^T\right)^\vee, \\ e_\Omega = \Omega - \Omega_d. \end{cases} \tag{9}$$

The error dynamic equation is as follows

$$\begin{cases} \dfrac{d}{dt}\phi(R_e) = e_R \cdot (R_d e_\Omega), \\ \dot{e}_R = Ee_\Omega, \\ \dot{e}_\Omega = J^{-1}(u + d_\Omega - \Omega \times J\Omega) - \dot{\Omega}_d, \end{cases} \tag{10}$$

where

$$E = \frac{1}{2\sqrt{1 + tr\left(RR_d^T\right)}} \left(tr\left(R_d R^T\right) I - R_d R^T + 2e_R e_R^T\right) R_d. \tag{11}$$

3. Adaptive Terminal Sliding Mode Fault-Tolerant Controller Design on SO(3)

The system actuator is affected by the uncertainty of system parameters and external interference when the spacecraft performs the mission in space, which may cause the spacecraft attitude actuator to fail and make the spacecraft deviate from the desired attitude. In order to solve this problem, the controller design will be derived in this section from two cases of spacecraft attitude actuator failure before and after failure.

3.1. Situation 1 Terminal Sliding Mode Controller Design when no Actuator Failure Occurs. First, the sliding mode surface is constructed as follows:

$$s = \mathrm{k}_1 R_\mathrm{d}^\mathrm{T} e_R \|e_R\|^{m_0} + e_\Omega, \tag{12}$$

where k_1 and m_0 are constants greater than 0. The derivative of Equation (12) is

$$\dot{s} = \beta + \dot{e}_\Omega, \tag{13}$$

where

$$\beta = \mathrm{k}_1 \dot{R}_d^T e_R \|e_R\|^{\mathrm{m}_0} + \mathrm{k}_1 R_d^T \dot{e}_R \|e_R\|^{\mathrm{m}_0} + \mathrm{m}_0 \mathrm{k}_1 R_d^T e_R \|e_R\|^{\mathrm{m}_0 - 1}. \tag{14}$$

The control rate of this section is designed as follows:

$$u = J\left(-\mathrm{k}_2 s - \beta + \dot{\Omega}_\mathrm{d}\right) + \Omega \times J\Omega - \varepsilon \ \mathrm{sign}\ (s), \tag{15}$$

where ε is a constant greater than zero. $\mathrm{sign}\ (s) = [\mathrm{sgn}\ (s(1)), \mathrm{sgn}\ (s(2)), \mathrm{sgn}\ (s(3))]^T$.

Theorem 1. *Under the action of the control rate of Equation (15), the system error can converge to 0. At this time, the system reaches stability.*

Proof. (1) Firstly, it is proved that the systematic error will converge to 0 when the sliding mode surface s converges to 0.

The first Lyapunov function is selected as follows:

$$V_1 = \phi(R_e), \tag{16}$$

According to Equation (10), the derivative of Equation (16) is

$$\dot{V}_1 = e_R \cdot (R_d e_\Omega). \tag{17}$$

When the sliding mode surface $s = 0$, there is

$$e_\Omega = -\mathrm{k}_1 R_{\mathrm{d}}^{\mathrm{T}} e_R \|e_R\|^{m_0}. \tag{18}$$

So there is

$$\begin{aligned} \dot{V}_1 &= e_R \cdot (R_d e_\Omega) = e_R \cdot \left(-R_d k_1 R_{\mathrm{d}}^{\mathrm{T}} e_R \|e_R\|^{m_0}\right) \\ &= e_R \cdot \left(-k_1 e_R \|e_R\|^{m_0}\right) = -k_1 \|e_R\|^{m_0+2} \le 0. \end{aligned} \tag{19}$$

So the systematic error will converge to 0. □

Proof. (2) In this part, it will be proved that s will converge to 0 when the control rate u is entered

The second Lyapunov function is chosen as

$$V_2 = \frac{1}{2} s^T s. \tag{20}$$

Combine Equation (10) with Equation (13), the derivative of Equation (20) is

$$\begin{aligned} \dot{V}_2 &= s^T \dot{s} = s^T (\beta + \dot{e}_\Omega) = s^T \left(\beta + J^{-1}(u + d_\Omega - \Omega \times J\Omega) - \dot{\Omega}_d\right) \\ &= s^T \begin{pmatrix} \beta + J^{-1} \begin{pmatrix} J\left(-\mathrm{k}_2 s - \beta + \dot{\Omega}_{\mathrm{d}}\right) \\ -\varepsilon sgn(s) + \\ d_\Omega + \Omega \times J\Omega \\ -\Omega \times J\Omega \end{pmatrix} \\ -\dot{\Omega}_d \end{pmatrix} \\ &= s^T \left(-k_2 s - J^{-1}(\varepsilon sgn(s) - d_\Omega)\right) \le -k_2 s^T s \le 0. \end{aligned} \tag{21}$$

The above equation holds when ε is sufficiently large. Therefore, the sliding mode surface s will converge to 0. In summary, the control rate designed in this section ensures that the system error will converge to 0, which means that the system remains stable when the spacecraft actuator does not fail. By now, Theorem 1 is proven. □

3.2. Situation 2 Adaptive Terminal Sliding Mode Fault-Tolerant Controller Design in Case of Actuator Failure. There are two main types of actuator faults: one is multiplicative and the other is additive. The control output of the former is related to the input, and the control output of the latter is not related to the input. And the actuator failure in most cases is mainly input-related [40]. Therefore, in this section, adaptive terminal fault-tolerant controller design is performed for actuator multiplicative faults. The control input in the event of a multiplicative fault is expressed as

$$u_c = \delta u, \tag{22}$$

where δ is the failure factor, when $\delta = 1$, the actuator does not fail, and when $\delta < 1$, the actuator fails. Therefore, the dynamic model and the error dynamic equation are updated as

$$\begin{cases} \dot{R} = R\widehat{\Omega}, \\ J\dot{\Omega} = -\Omega \times J\Omega + \delta u + d_\Omega, \end{cases} \tag{23}$$

$$\begin{cases} e_R = \dfrac{1}{2\sqrt{1 + tr(R_e)}} \left(R_e - R_e^T\right)^\vee, \\ e_\Omega = \Omega - \Omega_d, \end{cases} \tag{24}$$

$$\begin{cases} \dfrac{d}{dt}\phi(R_e) = e_R \cdot (R_d e_\Omega), \\ \dot{e}_R = E e_\Omega, \\ \dot{e}_\Omega = J^{-1}(\delta u + d_\Omega - \Omega \times J\Omega) - \dot{\Omega}_d. \end{cases} \tag{25}$$

A new terminal sliding surface was designed as follows:

$$s_c = k_1 R_{\mathrm{d}}^{\mathrm{T}} e_R \|e_R\|^{m_0} + e_\Omega. \tag{26}$$

The derivative of Equation (26) is

$$\begin{aligned} \dot{s}_c &= \mathrm{k}_1 \dot{R}_d^T e_R \|e_R\|^{\mathrm{m}_0} + \mathrm{k}_1 R_d^T \dot{e}_R \|e_R\|^{\mathrm{m}_0} \\ &\quad + \mathrm{m}_0 \mathrm{k}_1 R_d^T e_R \|e_R\|^{\mathrm{m}_0 - 1} + \dot{e}_\Omega \\ &= \beta + \dot{e}_\Omega. \end{aligned} \tag{27}$$

Let $\rho = 1/\delta$, the adaptive terminal sliding mode fault-tolerant control rate is designed as follows:

$$u = -\rho_2 \alpha, \tag{28}$$

where $\alpha = J(\mathrm{k}_2 s + \beta - J^{-1}(\Omega \times J\Omega) - \dot{\Omega}_{\mathrm{d}}) + \varepsilon \operatorname{sign}(s)$ and ρ_2 denotes the estimated value of the actual value ρ. The adaptive rate is designed as

$$\dot{\rho}_2 = \gamma \operatorname{sgn} |\delta| s^{\mathrm{T}} J^{-1} \alpha, \tag{29}$$

where γ is a constant greater than 0.

Theorem 2. *Under the action of this adaptive terminal fault-tolerant control rate, the system error can converge to 0, and the system remains stable after the failure of the system actuator.*

Proof. (1) Firstly, it is proved that the system error will converge to 0 when the slipform surface s_c converges to 0.

The Lyapunov function is selected as follows:

$$V_3 = \phi(R_e). \tag{30}$$

According to Equation (25), the derivative of Equation (30) is

$$\dot{V}_3 = \frac{d}{dt}\phi(R_e) = e_R \cdot (R_d e_\Omega). \tag{31}$$

When $s_c = 0$, there is

$$e_\Omega = -k_1 R_{\mathrm{d}}^{\mathrm{T}} e_R \|e_R\|^{m_0}. \tag{32}$$

So, there is

$$\begin{aligned} \dot{V}_3 &= \frac{d}{dt}\phi(R_e) = e_R \cdot (R_d e_\Omega) \\ &= e_R \cdot \left(-R_d k_1 R_{\mathrm{d}}^{\mathrm{T}} e_R \|e_R\|^{m_0}\right) \\ &= -k_1 \|e_R\|^{m_0+2} \le 0. \end{aligned} \tag{33}$$

Therefore, the system error will tend to 0 when the sliding surface s_c tends to 0. □

Proof. (2) In this part, the sliding mode surface s_c will converge to 0 under the action of adaptive terminal fault-tolerant control rate are proved

The Lyapunov function is chosen as follows:

$$V_4 = \frac{1}{2} s_c^T s_c + \frac{|\delta|}{2\gamma}\tilde{\rho}^2, \tag{34}$$

where $\tilde{\rho} = \rho_2 - \rho$ denotes the error between the estimated value ρ_2 and the actual value ρ Combine Equation (27) with Equation (29), the derivative of Equation (34) is

$$\begin{aligned} \dot{V}_4 &= s_c^T \dot{s}_c + \tilde{\rho}\delta s_c^T J^{-1}\alpha = s_c^T \dot{s}_c + \tilde{\rho}\delta s_c^T J^{-1}\alpha \\ &= s_c^T\left(\dot{s}_c + \tilde{\rho}\delta J^{-1}\alpha\right) = s_c^T\left(\beta + \dot{e}_\Omega + (\rho_2\delta - \rho\delta)J^{-1}\alpha\right) \\ &= s_c^T\left(\beta + J^{-1}(\delta u + d_\Omega - \Omega \times J\Omega) - \dot{\Omega}_{\mathrm{d}} + J^{-1}(-\delta u - \alpha)\right) \\ &= s_c^T\left(\beta + J^{-1}(\delta u + d_\Omega - \Omega \times J\Omega - \delta u - \alpha) - \dot{\Omega}_{\mathrm{d}}\right) \\ &= s_c^T\left(\beta + J^{-1}\left(d_\Omega - \Omega \times J\Omega - J\left(\mathrm{k}_2 s + \beta - J^{-1}(\Omega \times J\Omega) - \dot{\Omega}_{\mathrm{d}}\right) - \varepsilon\ \mathrm{sgn}\ (s)\right) - \dot{\Omega}_{\mathrm{d}}\right) \\ &= s_c^T\left(\beta + J^{-1}\left(d_\Omega - \Omega \times J\Omega - J\mathrm{k}_2 s - J\beta + (\Omega \times J\Omega) + J\dot{\Omega}_{\mathrm{d}}\right) - \varepsilon\ \mathrm{sgn}\ (s)\right) - \dot{\Omega}_{\mathrm{d}}\right) \\ &= s_c^T\left(\beta + J^{-1}d_\Omega - J^{-1}\Omega \times J\Omega - \mathrm{k}_2 s - \beta + J^{-1}(\Omega \times J\Omega) + \dot{\Omega}_{\mathrm{d}} - J^{-1}\varepsilon\ \mathrm{sgn}\ (s) - \dot{\Omega}_{\mathrm{d}}\right) \\ &= s_c^T\left(J^{-1}d_\Omega - \mathrm{k}_2 s - J^{-1}\varepsilon\ \mathrm{sgn}\ (s)\right) = s_c^T\left(-\mathrm{k}_2 s - J^{-1}(\varepsilon\ \mathrm{sgn}\ (s) - d_\Omega)\right) \le -\mathrm{k}_2 s_c^T s_c \le 0. \end{aligned} \tag{35}$$

It can be concluded that with the adaptive terminal fault-tolerant control rate, the sliding mode surface s_c will converge to zero. In conclusion, the adaptive terminal sliding mode fault-tolerant controller designed in this section can ensure the stability of the system after the failure of the system actuator. □

By the now, all controller stability is proven to be complete.

Table 1: Control parameters for simulation.

Parameters	Values	Parameters	Values
δ	0.00001	k_1	10
γ	500	k_2	50
m_0	1/12	ε	0.0006
t_T	10 s		

Table 2: Error situation table for three cases at 50 s.

Parameters	Case 1	Case 2	Case 3
ϕ	7.7730*e*-05	0.0686	7.7724*e*-05
$\|e_R\|$	0.0088	0.2597	0.0088
$\|e_\Omega\|$	0.0554	0.0627	0.0554

Remark 3. Controller parameters affect controller performance. Increasing k_1, k_2, and m_0 can reduce the convergence. Increasing γ can improve the sensitivity of adaptive. However, the initial control input will be large correspondingly.

4. Simulation Background and Numerical Simulation Result

An adaptive terminal sliding mode fault-tolerant control approach to design and validate spacecraft attitude tracking is designed in this section. Attitude tracking simulation experiments are carried out to validate the effectiveness of the adaptive terminal sliding mode fault-tolerant method.

In order to verify the validity of the proposed method, three cases are set up, respectively. Case 1 represents the simulation of the sliding mode control when no faults occur. Case 2 represents the simulation of the sliding mode control when faults occur. Case 3 represents the simulation of the adaptive terminal sliding mode fault-tolerant control when fault occurs.

The initial and the desired attitude of the spacecraft is described by the exponential coordinate x of SO(3) which can be found in Equation (A.1) from Appendix A.

The initial attitude of the spacecraft is given by $x = 0.6\,\pi[-1.6 \quad 2 \quad 1]^T$. The initial angular velocity of the spacecraft is given by $\Omega = [0 \quad 0 \quad 0]^T$. The spacecraft desired attitude is $x_d = [\pi \sin(0.01t) \quad 0.008t \quad \pi \sin(0.012t)]^T$, and the mass and moment of inertia of the spacecraft are $m = 56.7kg$ and $J = \mathrm{diag}\,(4.85 \quad 5.10 \quad 4.76)\mathrm{kg} \cdot \mathrm{m}^2$. The disturbance input of the system are assumed as

$$d_\Omega = \begin{bmatrix} 1 + \sin(\pi t/125) + \sin(\pi t/200) \\ 1 - \sin(\pi t/125) - \sin(\pi t/200) \\ 1 + \cos(\pi t/125) + \cos(\pi t/200) \end{bmatrix} 10^{-5} N \cdot m. \tag{36}$$

Assuming a simulation time of 50 seconds and a malfunction in the attitude actuator occurring at time t_T, the

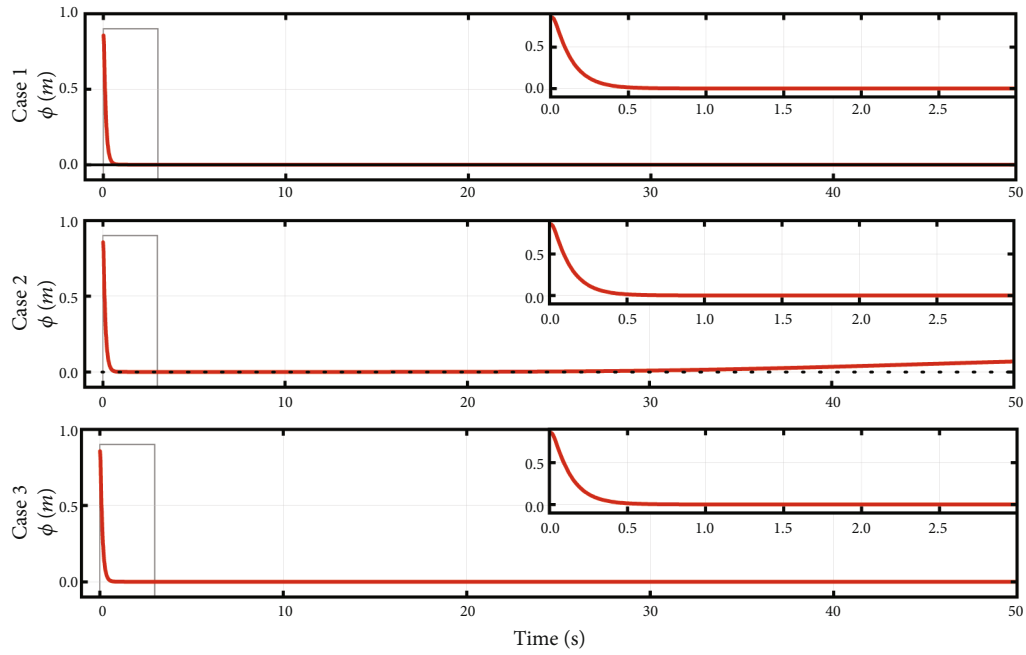

Figure 2: Time-dependent variation of attitude tracking error scalar.

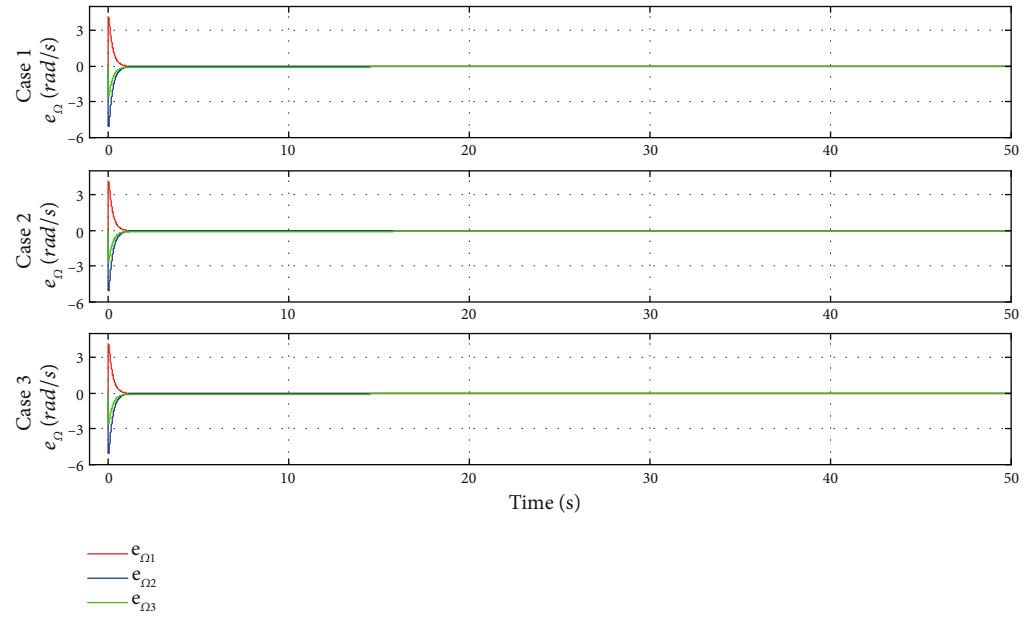

Figure 3: Time-dependent variation of angular velocity tracking error vector.

method presented in this study is able to immediately detect and respond to the fault without considering the potential effects of time delays in the system. The simulation parameters are shown in Table 1. Furthermore, the results for three cases at 50 seconds are presented in Table 2.

Figures 2–5 illustrate the curves of error parametrization, angular velocity, attitude, and input variation in the simulation experiment.

Figure 2 illustrates the variation of the spacecraft's attitude error scalar over time. In case 1, the error parametrization converges to zero within 1 second. This indicates effective tracking of the desired attitude trajectory by the control system. In case 2, when using sliding mode control with faults, the spacecraft converges to zero when t is less than 10 seconds. However, when a fault occurs at $t = 10$ seconds, the convergence curve diverges and fails to reach zero. This indicates the control system's vulnerability to faults and its inability to maintain stability. In case 3, the attitude error scalar converges to zero within 1 second. By implementing the fault-tolerant control method, the spacecraft can maintain stability and converge to zero even when a fault occurs at 10 seconds. This indicates the effective

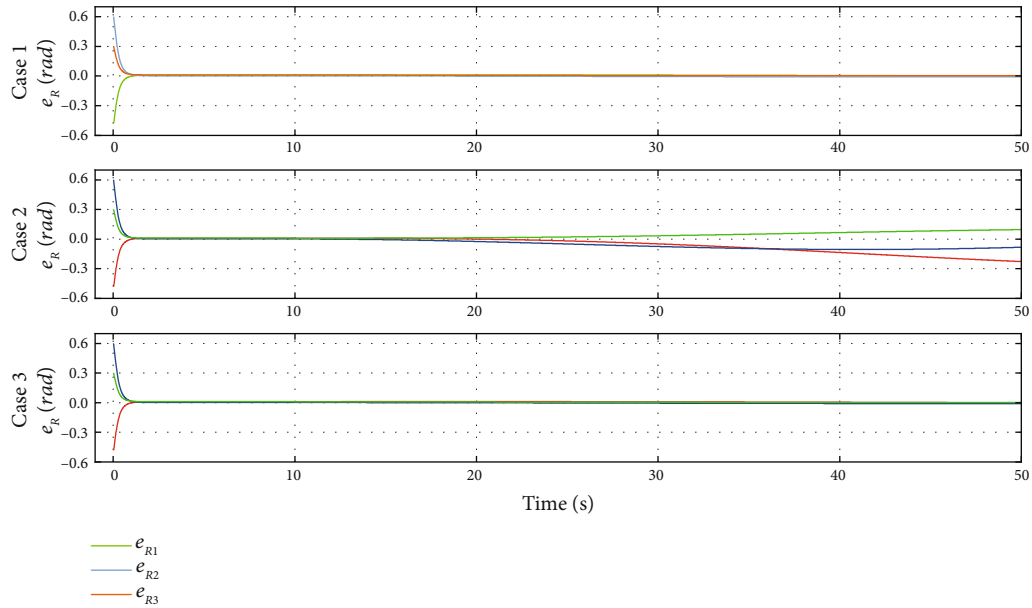

Figure 4: Time-dependent variation of attitude tracking error vectors.

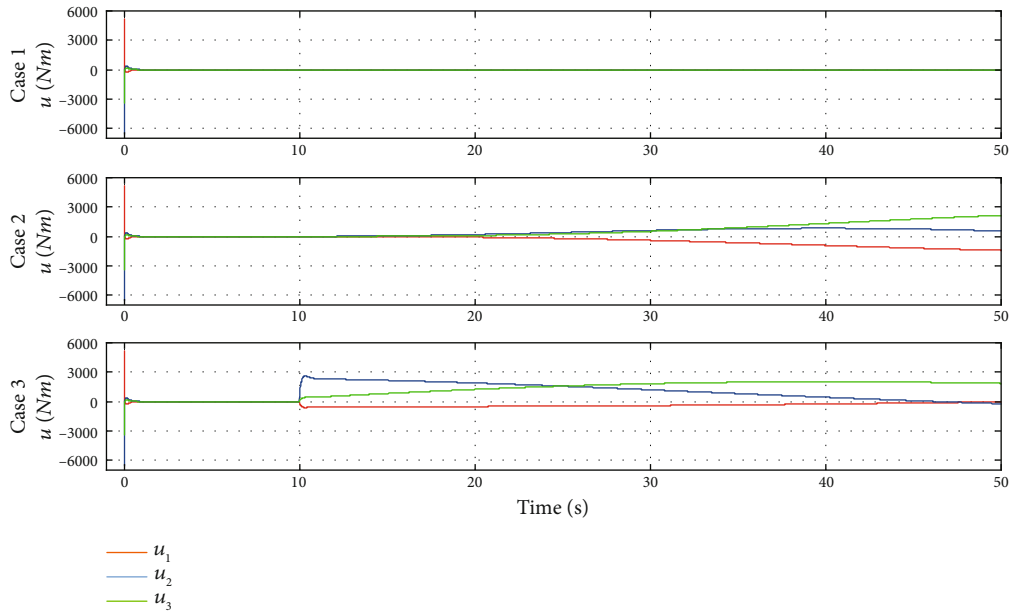

Figure 5: Time-dependent variation of the control input.

mitigation of fault impacts and stability maintenance by the fault-tolerant control method.

Figure 3 illustrates the variation of the spacecraft's angular velocity error vector over time. In case 1, case 2, and case 3, the angular velocity error vector converges to zero within 1 second. This indicates successful tracking of the desired angular velocity trajectory by the control system.

Figure 4 illustrates the variation of the spacecraft's attitude error vector over time. In case 1, the attitude error vector converges to zero within 1 second. In case 2, when using sliding mode control with faults, the spacecraft converges to zero when t is less than 10 seconds. However, when a fault occurs at $t = 10$ seconds, the convergence curve diverges and fails to reach zero. In case 3, the attitude error vector converges to zero within 1 second. By implementing the fault-tolerant control method, the spacecraft can maintain stability and converge to zero even when a fault occurs at 10 seconds. Conversely, case 3 demonstrates the effectiveness of the fault-tolerant control method, as the attitude error vectors converge to zero within 1 second despite the fault, showcasing stable and accurate attitude tracking.

Figure 5 illustrates the time-dependent variation of the spacecraft's input. The input converges to a small vibration near zero after the error converges, due to the slow rotation

of the desired attitude trajectory. In case 1, the input converges to a small vibration near zero within 1 second. In case 2, the input of the spacecraft converges to a slight vibration near zero before the failure occurs at t less than 10 seconds. However, after a fault occurs at $t = 10$ seconds, the convergence curve disperses and does not remain stable. In case 3, with the fault-tolerant control method, the input rapidly increases after a fault occurs to ensure the stability of error tracking. In contrast, case 3 demonstrates rapid increases in the input with the fault-tolerant control method to ensure the stability of error tracking after the fault occurrence. This demonstrates the fault-tolerant control method's ability to adapt and compensate for faults, ensuring stability in the control input.

In summary, Figures 2–5 present a comprehensive analysis of the control system's performance in various scenarios. The results emphasize the effectiveness of the adaptive terminal sliding mode fault-tolerant control method (case 3) in maintaining stability and accurate tracking of attitude, angular velocity, and control input, even in the presence of faults. These findings demonstrate the potential of the proposed control method for real-world applications, where faults and disturbances are likely to occur, ensuring the robustness and reliability of the control system.

5. Conclusions

To solve the problem of spacecraft attitude actuator fault, an ATSMFTC based on differential manifold SO(3) modelling is designed in this paper. First, SO(3) is used to provide a global and unique description of spacecraft attitude dynamics. This modelling method not only avoids the problems of fuzziness and unwinding existing in traditional modelling methods but also provides a simple expression of the dynamic equation of SO(3) modelling. Then a left attitude error description function is constructed on SO(3) to design an ATSMFTC. The controller can track the time-varying desired attitude quickly and accurately. At the same time, when the spacecraft attitude actuator fails, it can react quickly to keep the system stable. The controller designed based on the left attitude error description system of SO(3) has the characteristics of small computation and a simple design process. Finally, the practicability and scientificity of the controller are verified by numerical simulation. It can provide theoretical support for practical engineering applications such as spacecraft rendezvous and docking, formation flight, and asteroid companion flight. Through rigorous numerical simulation analysis, the control scheme designed in this paper can be realized in practical engineering applications.

Appendix

A. Exponential Map

For the Lie groups SO(3), their Lie algebra so(3), the exponential is defined below [37] and [41, 42].

Table 3: Nomenclature.

Name	Implication
$SO(3)$	The differential manifold
R	The attitude
I	Identity matrix
Ω	The angular velocity
J	The rotational moment of inertia
u	The total control torque
d_Ω	An unknown random disturbance
R_d	The desired attitude
$R_{e,l}$	The left error function
$R_{e,r}$	The right error function
φ	The error function
ϕ	The error parametrization
e_R	The attitude error vector
Ω_d	The desired angular velocity
e_Ω	The angular velocity error vector
s	The sliding mode surface
k_1	The controller parameter
m_0	The controller parameter
k_2	The controller parameter
ε	A constant
u_c	The control input in the event of a multiplicative fault
δ	The failure factor
s_c	The sliding mode surface
ρ	Reciprocal of δ
α	Adaptive rate parameter
ρ_2	The estimated value of the actual value ρ
γ	A constant greater than 0
$\tilde{\rho}$	The error between ρ_2 and ρ
t_T	Time of failure

Lemma A.1. *Given any Lie algebra $\hat{x} \in so(3)$, the map $\exp_{SO(3)} : so(3) \longrightarrow SO(3)$ is defined as*

$$\exp_{SO(3)}(\hat{x}) = I + \frac{\sin \|x\|}{\|x\|}\hat{x} + \frac{1 - \cos \|x\|}{\|x\|^2}\hat{x}^2, \tag{A.1}$$

where $\|\cdot\|$ is the standard Euclidean norm. (A.1) is the Rodrigues' formula $\|x\| < \pi$ and $x/\|x\|$ represent the rotation angle and axis between R and I_3. $x \in \mathbb{R}^3$ is the exponential coordinates of Lie groups SO(3).

B. Table of Nomenclature

All the terms in this article are represented in Table 3.

Data Availability

The authors confirm that the data supporting the findings of this study are available within the article.

Conflicts of Interest

The authors declare that they have no conflicts of interest.

Acknowledgments

Funding support by the Collaborative Innovation Center of Intelligent Green Manufacturing Technology and Equipment, Shandong (IGSD-2020-007) is gratefully acknowledged.

References

[1] Y. Wang and H. Ji, "Integrated relative position and attitude control for spacecraft rendezvous with ISS and finite-time convergence," *Aerospace Science and Technology*, vol. 85, pp. 234–245, 2019.

[2] K. Xia and W. Huo, "Robust adaptive backstepping neural networks control for spacecraft rendezvous and docking with input saturation," *ISA Transactions*, vol. 62, pp. 249–257, 2016.

[3] G. Klančar, S. Blažič, D. Matko, and G. Mušič, "Image-based attitude control of a remote sensing satellite," *Journal of Intelligent and Robotic Systems*, vol. 66, no. 3, pp. 343–357, 2012.

[4] B. Shahbazi, M. Malekzadeh, and H. R. Koofigar, "Robust constrained attitude control of spacecraft formation flying in the presence of disturbances," *IEEE Transactions on Aerospace and Electronic Systems*, vol. 53, no. 5, pp. 2534–2543, 2017.

[5] D. Lee, J. E. Cochran Jr., and T. S. No, "Robust position and attitude control for spacecraft formation flying," *Journal of Aerospace Engineering*, vol. 25, no. 3, pp. 436–447, 2012.

[6] C. Gao, Q. Zhao, and G. Duan, "Robust actuator fault diagnosis scheme for satellite attitude control systems," *Journal of the Franklin Institute*, vol. 350, no. 9, pp. 2560–2580, 2013.

[7] S. Ahmad, A. A. Uppal, M. R. Azam, and J. Iqbal, "Chattering free sliding mode control and state dependent Kalman filter design for underground gasification energy conversion process," *Electronics*, vol. 12, no. 4, p. 876, 2023.

[8] Q. Hu, B. Xiao, and M. I. Friswell, "Robust fault-tolerant control for spacecraft attitude stabilisation subject to input saturation," *IET Control Theory Applications*, vol. 5, no. 2, pp. 271–282, 2011.

[9] Y. Han, J. D. Biggs, and N. Cui, "Adaptive fault-tolerant control of spacecraft attitude dynamics with actuator failures," *Journal of Guidance, Control, and Dynamics*, vol. 38, no. 10, pp. 2033–2042, 2015.

[10] S. Yin, B. Xiao, S. X. Ding, and D. Zhou, "A review on recent development of spacecraft attitude fault tolerant control system," *IEEE Transactions on Industrial Electronics*, vol. 63, no. 5, pp. 3311–3320, 2016.

[11] Q. Hu, B. Jiang, and Z. Shi, "Novel terminal sliding mode based fault tolerant attitude control for spacecraft under actuator faults," *Acta Aeronautica et Astronautica Sinica*, vol. 35, no. 1, pp. 249–258, 2014.

[12] M. N. Hasan, M. Haris, and S. Qin, "Finite-time active fault-tolerant attitude control for flexible spacecraft with vibration suppression and anti-unwinding," *Advances in Space Research*, vol. 71, no. 9, pp. 3644–3660, 2023.

[13] Q. Hu, A. Zhang, and B. Li, "Adaptive variable structure fault tolerant control of rigid spacecraft under thruster faults," *Acta Aeronautica ET Astronautica Sinica*, vol. 34, no. 4, pp. 909–918, 2013.

[14] S. M. Esmaeilzadeh, M. Golestani, and S. Mobayen, "Chattering-free fault-tolerant attitude control with fast fixed-time convergence for flexible spacecraft," *International Journal of Control, Automation and Systems*, vol. 19, no. 2, pp. 767–776, 2021.

[15] X. Shao, Q. Hu, Y. Shi, and Y. Zhang, "Fault-tolerant control for full-state error constrained attitude tracking of uncertain spacecraft," *Automatica*, vol. 151, article 110907, 2023.

[16] Y. Yang, "Spacecraft attitude determination and control: quaternion based method," *Annual Reviews in Control*, vol. 36, no. 2, pp. 198–219, 2012.

[17] R. Kristiansen and P. J. Nicklasson, "Satellite attitude control by quaternion-based backstepping," in *Proceedings of the 2005, American Control Conference, 2005*, pp. 907–912, Portland, OR, USA, June 2005.

[18] W. Shang, G. Jing, D. Zhang, T. Chen, and Q. Liang, "Adaptive fixed time nonsingular terminal sliding-mode control for quadrotor formation with obstacle and inter-quadrotor avoidance," *IEEE Access*, vol. 9, no. 9, pp. 60640–60657, 2021.

[19] W. Shang, G. Jing, Y. Wang, T. Chen, Z. Liu, and Z. Zheng, "Adaptive prescribed time control for quadrotor formation with stochastic links failure," *Asian Journal of Control*, vol. 25, no. 4, pp. 2699–2719, 2023.

[20] A. Gray, *A Treatise on Gyrostatics and Rotational Motion*, Macmillan, New York, USA, 1918.

[21] H. Schaub and J. L. Junkins, "Stereographic orientation parameters for attitude dynamics: a generalization of the Rodrigues parameters," *Journal of the Astronautical Sciences*, vol. 44, no. 1, pp. 1–19, 1996.

[22] R. Gupta, U. V. Kalabić, S. Di Cairano, A. M. Bloch, and I. V. Kolmanovsky, "Constrained spacecraft attitude control on SO(3) using fast nonlinear model predictive control," in *2015 American Control Conference (ACC)*, pp. 2980–2986, Chicago, IL, USA, July 2015.

[23] U. V. Kalabić, R. Gupta, S. Di Cairano, A. M. Bloch, and I. V. Kolmanovsky, "MPC on manifolds with an application to the control of spacecraft attitude on SO(3)," *Automatica*, vol. 76, pp. 293–300, 2017.

[24] Z. H. Ning, C. H. Xiaodong, X. I. Yuanqing, H. U. Jie, and W. A. Qiping, "Quaternion-based fault-tolerant control design for spacecraft attitude stabilization: an anti-saturation method," in *2019 Chinese Control Conference (CCC)*, pp. 2558–2563, Guangzhou, China, July 2019.

[25] W. Cai, X. H. Liao, and Y. D. Song, "Indirect robust adaptive fault-tolerant control for attitude tracking of spacecraft," *Journal of Guidance, Control, and Dynamics*, vol. 31, no. 5, pp. 1456–1463, 2008.

[26] J. D. Boskovic, S. M. Li, and R. K. Mehra, "Fault tolerant control of spacecraft in the presence of sensor bias," in *Proceedings of the 2000 American Control Conference. ACC (IEEE Cat. No. 00CH36334)*, pp. 1205–1209, Chicago, IL, USA, June 2000.

[27] Q. Hu, B. Xiao, and M. I. Friswell, "Fault tolerant control with H∞ performance for attitude tracking of flexible spacecraft," *IET Control Theory and Applications*, vol. 6, no. 10, pp. 1388–1399, 2012.

[28] S. P. Bhat and D. S. Bernstein, "A topological obstruction to continuous global stabilization of rotational motion and the unwinding phenomenon," *Systems Control Letters*, vol. 39, no. 1, pp. 63–70, 2000.

[29] M. D. Shuster, "A survey of attitude representations," *Navigation*, vol. 8, no. 9, pp. 439–517, 1993.

[30] X.-N. Shi, D. Zhou, X. Chen, and Z.-G. Zhou, "Actor-critic-based predefined-time control for spacecraft attitude formation system with guaranteeing prescribed performance on SO(3)," *Aerospace Science and Technology*, vol. 117, article 106898, 2021.

[31] U. Kalabić, R. Gupta, S. Di Cairano, A. Bloch, and I. Kolmanovsky, "Constrained spacecraft attitude control on SO(3) using reference governors and nonlinear model predictive control," in *2014 American Control Conference*, Portland, OR, USA, June 2014.

[32] T. Lee, "Relative attitude control of two spacecraft on SO(3) using line-of-sight observations," in *2012 American Control Conference (ACC)*, pp. 167–172, Montreal, QC, Canada, June 2012.

[33] Q. Meng, H. Yang, and B. Jiang, "Second-order sliding-mode on SO(3) and fault-tolerant spacecraft attitude control," *Automatica*, vol. 149, article 110814, 2023.

[34] Y. Mei, Y. Liao, K. Gong, and D. Luo, "Fuzzy adaptive sliding mode fault estimation and fixed-time fault-tolerant control for coupled spacecraft based on SE(3)," *Aerospace Science and Technology*, vol. 126, article 107673, 2022.

[35] F. Bullo and R. M. Murray, "Tracking for fully actuated mechanical systems: a geometric framework," *Automatica*, vol. 35, no. 1, pp. 17–34, 1999.

[36] T. Lee, "Exponential stability of an attitude tracking control system on SO(3) for large-angle rotational maneuvers," *Systems Control Letters*, vol. 61, no. 1, pp. 231–237, 2012.

[37] Y. Wang, H. Hong, and S. Tang, "Geometric control with model predictive static programming on SO(3)," *Acta Astronautica*, vol. 159, pp. 471–479, 2019.

[38] Y. Wang, S. Tang, J. Guo, X. Wang, and C. Liu, "Fuzzy-logic-based fixed-time geometric backstepping control on SO(3) for spacecraft attitude tracking," *IEEE Transactions on Aerospace and Electronic Systems*, vol. 55, no. 6, pp. 2938–2950, 2019.

[39] M. B. Anjum, Q. Khan, S. Ullah et al., "Maximum power extraction from a standalone photo voltaic system via neuro-adaptive arbitrary order sliding mode control strategy with high gain differentiation," *Applied Sciences*, vol. 12, no. 6, p. 2773, 2022.

[40] K. Ali, A. Mehmood, and J. Iqbal, "Fault-tolerant scheme for robotic manipulator–nonlinear robust back-stepping control with friction compensation," *PLoS One*, vol. 16, no. 8, article e0256491, 2021.

[41] F. Bullo and R. M. Murray, *Proportional derivative (PD) control on the Euclidean group*, California Institute of Technology, 1995.

[42] Z. Zheng, W. Shang, J. Ai, Y. Zou, and Z. Liu, "Integrated geometric optimal control of spacecraft attitude and orbit based on *SE*(3)," *IEEE Access*, vol. 11, pp. 27382–27394, 2023.